Proceedings of the Twenty-sixth (2016) International Ocean and Polar Engineering Conference **www.isope.org**
Rhodes, Greece, June 26-July 1, 2016

ISBN 978-1-880653-88-3; ISSN 1098-6189

GIS Mapping of Fluid Mud Transport Pre-, During-, and Post-Dredging Agitation, by using Engineered Novel Instrumentation

Tyler A. Rotkiske, Charles R. Bostater, Jr.,
Marine and Environmental Lab, College of Engineering
Florida Institute of Technology Melbourne, FL, USA

ABSTRACT

A methodology that utilizes georeferenced imagery to analyze spatial fluid mud flux measurements pre-, during-, and post-dredging is described. The spatial analysis technique utilizes novel passive sonde sampling techniques and above surface imagery in ArcGIS to geometrically represent fluid mud flux over a specific area of the dredging project waterway. Transect data obtained from the Indian River Lagoon (IRL), south of Sebastian Inlet, Florida is used to mathematically calculate combined fluid mud and flocculation transport in the North, South, East, West, settling (depositional), and upwelling (resuspension) directions across the navigable marine channel at four transects. Satellite imagery is transferred into raster images using ten point image to image georeferencing technique and a 3rd order image transformation providing a root mean square error of < 0.1 m. A kriging technique coupled with contouring was utilized to give a spatial representation of the point sampling data between sampling stations. Digitization of the water area is essential in order to calculate the flux over the surface area of the nearby estuary. The advantages of these techniques are the estimation of fluid mud movement over an estuarine region given sonde data during the dredging of waterways in coastal areas. The techniques are transferrable to other water bodies.

KEY WORDS: fluid mud; particle settling; lutocline; sonde; GIS mapping; estuary; dredging; particle resuspension.

INTRODUCTION

Dredging operations result in the suspension of fine grained sediments decreasing the amount of light that passes through the water column to the seafloor. A large portion of the fine grained materials that are suspended off the bottom remain in a turbid lutocline for extended periods of time. Sediments that are entrained in the lutocline are referred to as fluid mud. The suspension of fluid mud results in the reduction of subsurface irradiance throughout these periods potentially resulting in detrimental effects to the benthic aquatic life that rely on light for vision and productivity (Aumack et al., 2007). In areas where a fluid mud bottom type is dominated, dredging can cause turbulence, suspending and breaking apart the lutocline material. In order for these particles to settle once again they must undergo cohesion between other fine grained particles until the density is large enough to result in a floc to settle out (Winterwerp, 2002). Settling velocities of fluid mud are on the order of 10^{-1} mm s^{-1}, significantly slower than the tidal current speeds that are encountered. According to Vinzon and Mehta (2003) current *in-situ* methods used to gain an insight into the mass transport have difficulties measuring concentrations greater than (1 – 2 kg m^{-3}). Due to these difficulties in sampling suspended concentrations, typical sampling is performed instantaneously. This water sampling however, does not include estimates of directional particulate fluxes (g m^{-2} s^{-1}). McNally et al, 2007 indicates that flux measurements require sampling to be integrated over time. *In-situ* passive sonde sampling techniques used by Bostater & Rotkiske (2015) measure the mass flux (g) that moves through a sampling area of the sonde during a deployment period. This method is the only reported direct method for flux conserving measurements of moving fluid mud and muck.

Geographic Information Systems (GIS) is a powerful tool that can be used advantageously to represent particulate flux data, temporally and spatially as well. GIS has the ability to determine and develop relationships that otherwise may not be seen and explored with more common graphical methods. When modeling directional particulate fluxes, GIS can be used to view large amounts of data and even better, to determine spatiotemporal distributions through the use of statistical kriging methods. This data can be used for model inputs used to determine sediment fluxes. Rennie and Church (2010) suggest that kriging methods can provide mathematical and statistical spatial smoothing technique that improves the visual representation caused by the errors in measurements. The reliability of the kriging model is a function of the frequency of sampling distributed over the study site. Since fluid mud fluxes cannot be represented or estimated through instantaneous sampling, difficulties become present in collecting enough sampling data to reliably determine the sediment fluxes throughout the entire extents of the estuary. Therefore, representations of sediment fluxes have only been represented for the channel.

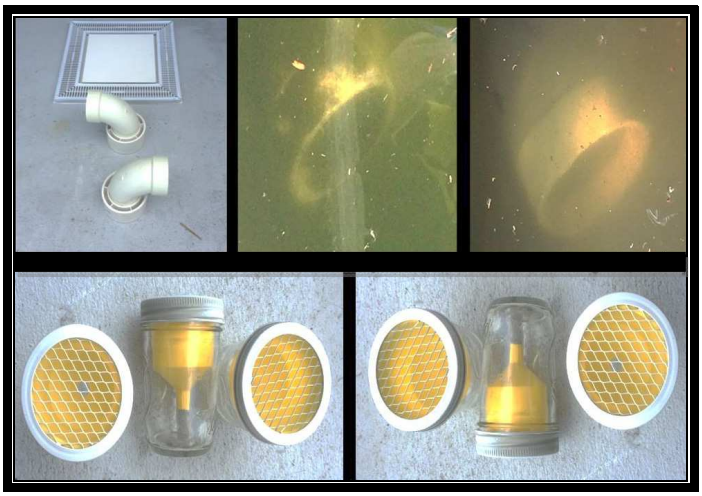

Figure 1: In the top left image horizontal sondes are pictured. The top center image shows a horizontal sonde that has been deployed over an 12 hour period. The top right shows a horizontal sonde at initial deployment. The bottom two images show the vertical sondes (from Bostater and Yang, 2014).

METHODS

The sonde deployment periods were pre-, during-, and after-dredging operations. Sondes are used for fluid mud sampling vertically and horizontally. They were first discussed by Bostater and Yang (2014) and mentioned by DiToro in 2001. Horizontal and vertical sondes shown in Fig. 1 were fabricated in order to capture fine grain sediments and flocs moving in different directions. Four cross sectional transects were randomly selected in the Indian River Lagoon (IRL), between the Wabasso Bridge, FL and the southeastern side of the Sebastian Inlet. Each cross sectional transect consisted of three duplicate sets of horizontal and vertical sondes across the channel, with one set in the channel and two sets outside of the channel. At the initial deployment, horizontal and vertical sondes were capped while being secured to the bottom to prevent errors in measurement of fluid mud transport. Once sondes were secured to the bottom, the caps were removed. Placement of the horizontal sondes was 3 m apart in the North, South, East, and West directions, respectively. Duplicate sets of vertical sondes were place upright and inverted at 10 cm above the bottom and 50 cm above the bottom, which can be seen in Fig. 2. Sondes were left in the water over an approximate 12 hour period and retrieved. Before their retrieval, the sondes were capped and then removed from the bottom and the time recorded.

Samples were allowed to settle in a lab for 48 hours and water was decanted from the top of the sample and rinsed with deionized water. The sample was transferred to a small crucible where the wet weight and volume were recorded. The sample was allowed to settle for 48 hours. Water was decanted and the sample was dried at 100˚C for 24 hours, in order to obtain a dry weight. By using standard methods, the ash weight was determined and the inorganic weight and organic weight calculated for each sample by using a furnace at 550°C.

Control links were established at the four corners of the satellite image of the study area and were georeferenced via a spline transformation to give a root mean square error of less than 1 m. Using image to image georeferencing, control points were established between an image of the study area and a georeferenced Google map. A 3rd order transformation was performed to give a root mean square error of 0.0003 meters.

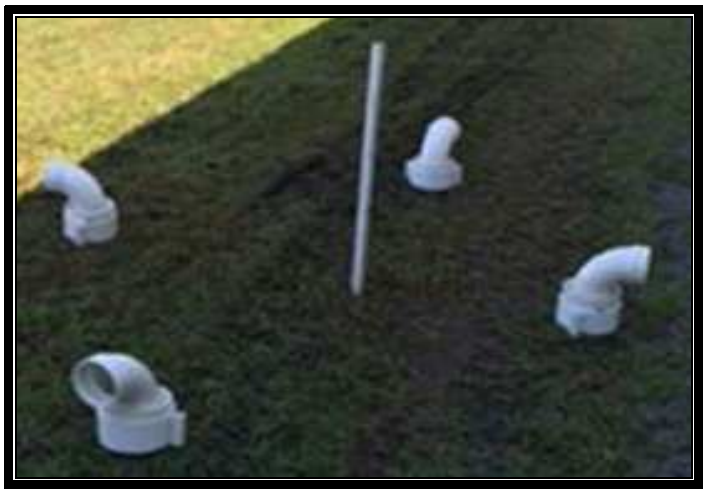

Figure 2: Mock directional orientation of the horizontal and vertical sonde set up at each location.

The dry weight flux g m^{-2} min^{-1} can be calculated in the GIS attributes table by dividing the dry weight of the collected sonde deposit (g) by the cross sectional area of the sonde (m^2) divided by the time (s). Data from sampling and flux measurements were displayed through the world geodetic system 1984 in decimal degrees. Using a query by location the pre-, during-, and post-flux calculations were separated into layers.

The study was limited to the cross sectional area of the dredged channel and a polygon shape file for the channel was created in order to limit the extents of the spatial distribution of the kriging method. This technique is known as masking or the limitation of the processing extents. A kriging method was run for pre-, during-, and post-dredging operations on the total dry weight fluxes that were integrated over the sampling period.

In order to represent the organic and wet weight percentages of each sonde, a pie-chart classification was created for the pre-, during-, and after-dredging operations. The representation of the organic and inorganic weights (of moving fluid mud) in this fashion leads to a spatial/graphical interpretation and understanding of how dredging influences the amount of fluid mud fluxes. A geographically weighted regression analysis was run between the deployment period and the dry weight fluxes to give a geographically weighted standard deviation (g m^{-2}) between points.

RESULTS

Prior to dredging, kriging was performed on the passive sediment dry weight fluxes in the horizontal and vertical directions (Fig. 3). The sediment fluxes were found to be between the range of 0.012 - 0.058 g m^{-2} min^{-1}. Transect 4 was mainly a sandy bottom type made up of particles which have cohesion-less properties allowing them to settle at larger velocities then the fine grained flocs (Winterwerp, 2002). The greater settling velocity results in less suspension of large grained particulate matter. Transect 3, which was also a sandy bottom type mixed with large rocks experienced low suspension of particulate matter. Transect 1 and 2 were mud bottoms which resulted in larger amounts of sediments that were suspended in the water column and became trapped in the vertical and horizontal sondes. The highest weighted depository flux was found to be 0.058 g m^{-2} min^{-1} at transect two.

Figure 3: Pre-dredging dry weight fluxes (g m^{-2} min^{-1}) in-between the Wabasso Bridge and South side of the Sebastian Inlet. Channel cross sections are labeled from South(1) to North(2). (Multispectral image: Courtesy of Digital Globe)

Figure 4: During-dredging dry weight fluxes (g m^{-2} min^{-1}) in-between the Wabasso Bridge and South side of the Sebastian Inlet. Channel cross sections are labeled from South(1) to North(2). (Multispectral image: Courtesy of Digital Globe)

During dredging operations, the depositional flux increased an order of magnitude to a range between 0.3 and 0.7 g m^{-2} min^{-1}. The kriging interpolation in (Fig. 4) shows that during dredging operations the flux remains uniform throughout the entire study area. This uniformity suggests a difference between the pre- and during-dredging operations.

After-dredging operations (Fig. 5) indicate that the levels of particulate flux remain within the same range, as found during-dredging. Particles or flocs that are suspended can be seen in (Fig. 7). The figure shows an intact water core with large flocs and suspended fine grained particles. Typically, these flocs break apart when they enter a sonde and settle. Thus the magnitude of moving flocks was previously unknown.

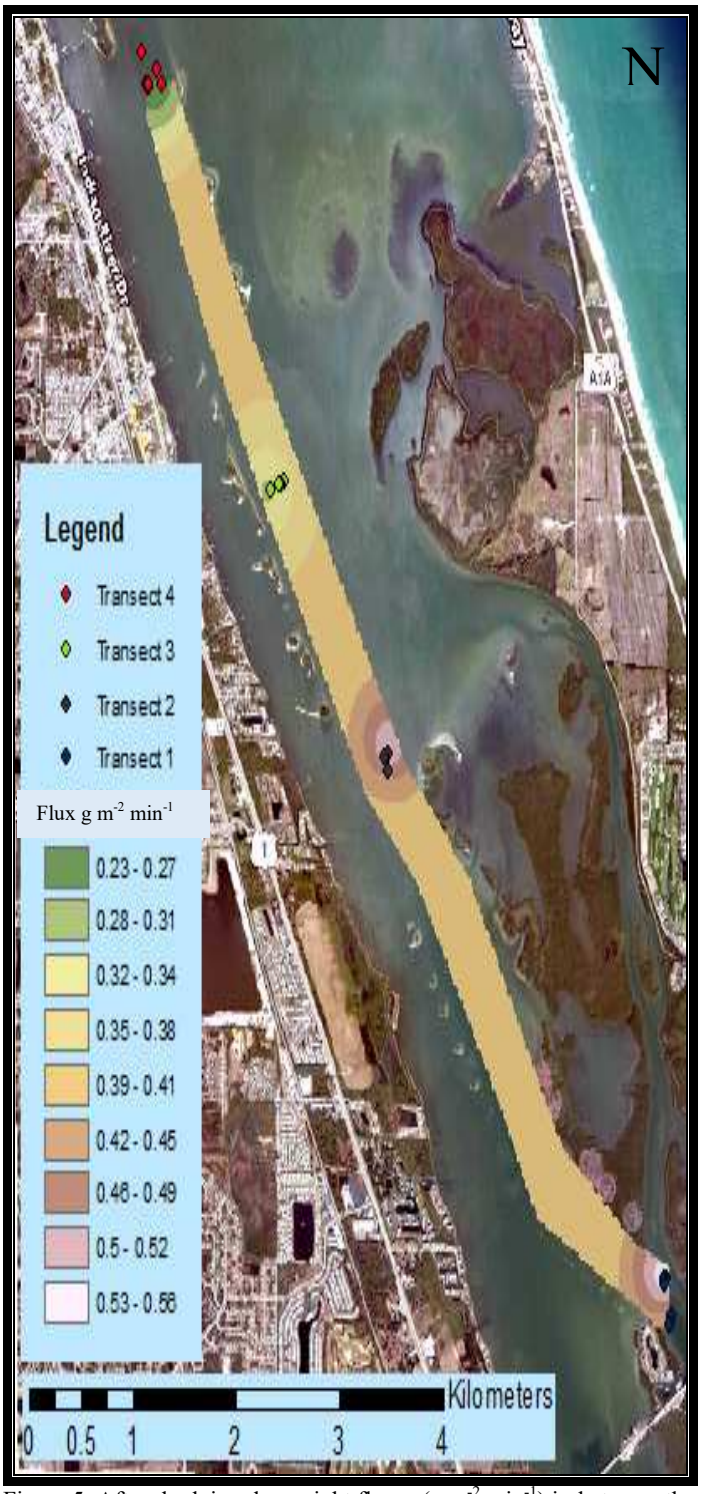

Figure 5: After-dredging dry weight fluxes (g m^{-2} min^{-1}) in-between the Wabasso Bridge and South side of the Sebastian Inlet. Channel cross sections are labeled from South(1) to North(2).

The percentage of inorganic and organic materials (Fig. 7) in the sonde pre-dredging, shows that inorganic materials mainly dominate the suspended material in the lutocline. During-dredging operations (Fig. 8) shows a dominance of organic suspended materials that were sampled. After-dredging (Fig. 9) shows mainly inorganic sediments that are suspended in lutocline layer of the water column. This indicates that as fine grained organic sediments remain suspended in the lutocline a large fracton fine grained inorganic particles settle out for removal. It suggests that during-dredging, fluid mud is removed resulting in the exhibition of greater amounts of the fine grained sediments that are inorganic. Finally, when dredging is completed, the organic materials appear to decrease due to the removal or relocated organics, due to turbulent fluctuaions cuased by dredging activities.

Figure 6: Water column core near the lutocline layer showing suspended fluid mud and flocks.

Transect 4 (Fig. 7) largely contained organic materials pre-dredging. During-dredging, the amount of organic materials increased, and then decreased to close to zero after dredging.

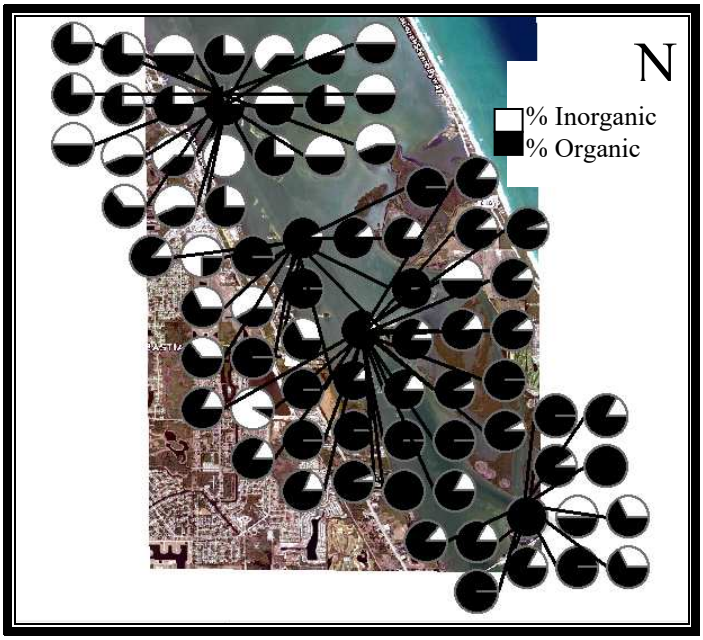

Figure 7: Pre-dredging percentage of particles collected in sonde that are organic and inorganic in-between Sebastian Inlet and the Wabasso Bridge throughout the channel. Lines from the pie-charts are associated with the transect location where sampling occurred.

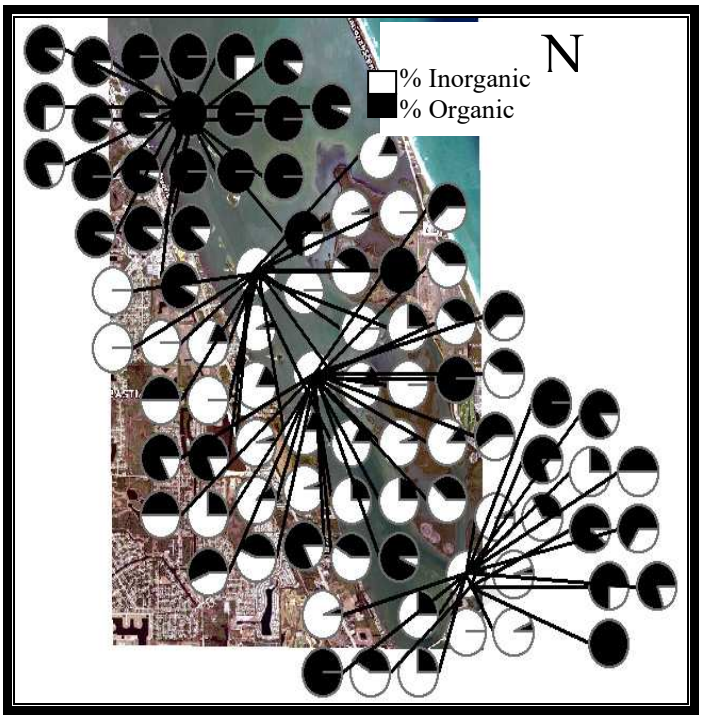

Figure 8: During dredging percent of particle's collected in-between Sebastian Inlet and the Wabasso Bridge throughout the channel. Inorganic and organic percentages are represented. Lines from the pie-charts are associated with the location in which sampling was taken.

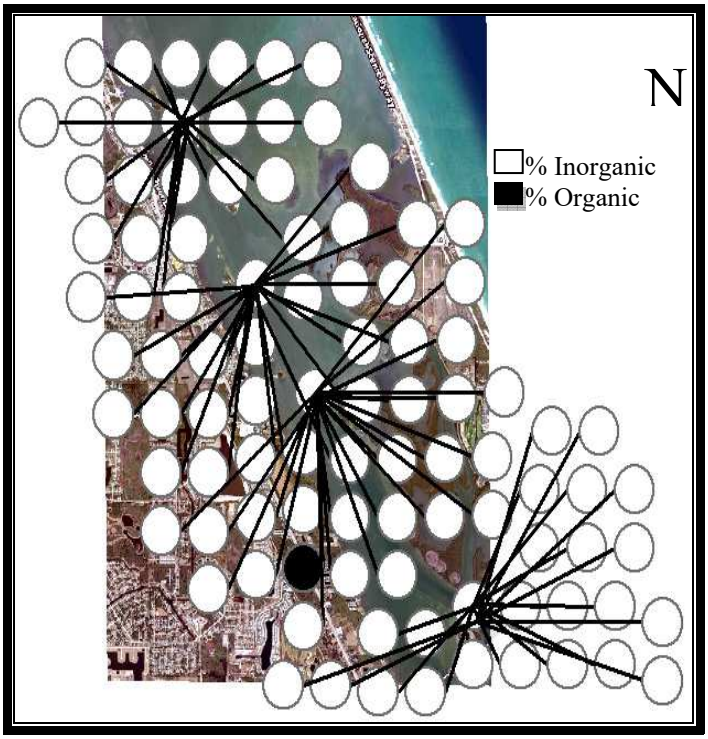

Figure 9: After-dredging percentage of particles collected in sonde that are organic and inorganic. Samples were collected in-between Sebastian Inlet and the Wabasso Bridge throughout the channel. Lines from the pie-charts are associated with the location in which sampling was taken. Four transects of sondes are represented.

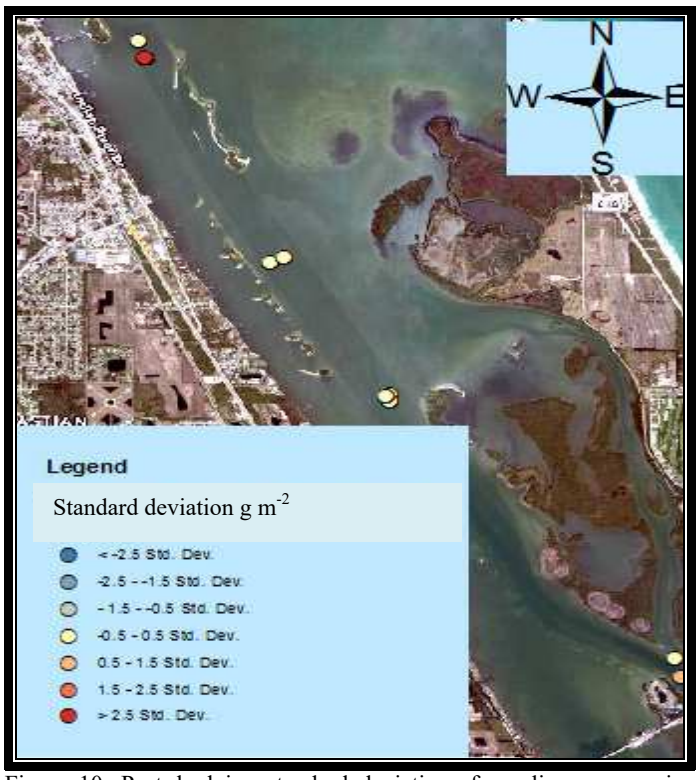

Figure 10: Post-dredging standard deviations for a linear regression between time and the depositional rate.

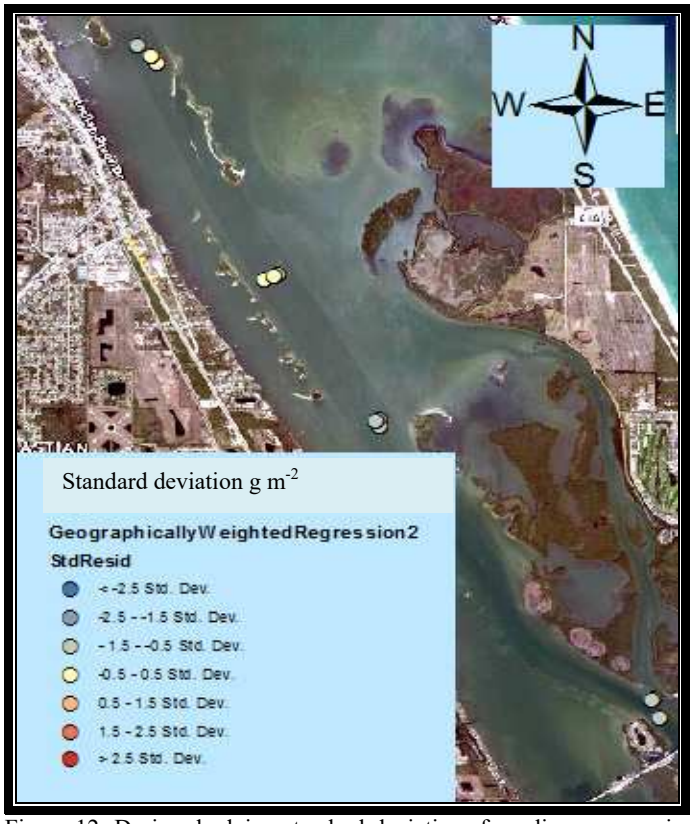

Figure 12: During-dredging standard deviations for a linear regression between time and the depositional rate.

Figure 11: Post-dredging standard deviations for a linear regression between time and the depositional rate.

The geographically weighted standard deviations for a linear regression between the dry weights recorded and the deployment time, are shown in (Figs.10 ~ 12). Data sampling is spread over a complex plane in the GIS, resulting in errors that cause negative standard deviations. Data suggests that the variations in the fluid mud flux was not due to the slight variations in the deployment time (±1 hr).

CONCLUSION

GIS techniques applied to dredging operations can be an extremely useful tool to use during decision making for evaluation of dredging efficacy. Kriging methods are a useful visual method to interpret the particulate flux distributions in estuaries such as the Indian River Lagoon. However, kriging methods assume diffusion-like processes are taking place between points as evidenced by decreasing particulate fluxes as one moves away from the sampling point as shown in (Fig, 6). Physically, wind, waves, and tidal currents result in the suspension of fluid mud. These random sediment fluctuations cannot be predicted through instantaneous point sampling. Passive sonde sampling is the only method that provides the ability to solve for the flux integrated over a sampling period.

The flux of fine grained particulate matter or fluid mud was found to increase during the dredging process. This increase persisted at same locations after dredging ceased. The data suggests that dredging removes large grained sedimentary surface layers resulting in increased suspension of fine grained fluid mud that is largely fine grained inorganic particulates.

From a statistical point of view, more sampling locations are needed to improve this research and in order to greatly improve the geospatial accuracy from kriging. Improvements are needed in instrumentation as well, in order to greatly reduce the time for the deployment and retrieval of sondes. One option might also be to create an array of sondes across the channel for passive sampling horizontally at multiple levels above the bottom. Such an approach would result in the creation of a three dimensional graphical interpretation of the channel cross sectional area fluxes for 3D predictions of sediment flux and transport modeling.

REFERENCES

Amuck, CF. et al (2007), *"Linking light attenuation and suspended sediment loading to benthic productivity within an artic kelp-bed community,"* Journal of Phycology, 43, 853-863.

Bostater, CR. Rotkiske, Tyler (2015), *"Moving fluid mud sondes, optical and acoustic sensing methods in support of coastal waterway dredging,"* Remote sensing of the Ocean, Sea Ice, Coastal Waters, and Large Water Regions", 9638, 1-17

DiToro, D (2001), *"Sediment Flux Modeling,"* John Wiley and Sons Ltd, US, 1-656.

McNally, W. et al (2007), *"Management of fluid mud in estuaries, bays, and lakes, I: Present State of understanding on character and behavior,"* Journal of Hydraulic Engineering, ASCE, 133, 9-22.

Rennie, CD. Church, M. (2010), *"Mapping spatial distributions and uncertainty of water and sediment flux in a large gravel bed river reach using an acoustic Doppler current profiler,"* Journal of Geophysical Research, 115, 1-27.

Bostater, C. Yang, B. (2014), "*Shallow Water Surface Gravity Wave Imaging, Spectra and Their Use in Shallow Water Dredging Operations*," Remote Sensing of the Ocean, Sea Ice, Coastal Waters, and Large Water Regions", 9240, 1-9.

Vinzon, S. Mehta, AJ (2003), "*Lutoclines in High Concentration Estuaries: Some Observations at the Mouth of the Amazon,"* Journal of Coastal Research, 19(2), 243-253.

Winterwerp, JC. (2002), "*On the flocculation and settling velocity of estuarine mud,"* Continental Shelf Research, 22(9), 1339-1360.